

Electronic Supplementary Information (ESI)

The Effect of Particle Size and Ligand Configuration on the Asymmetric Catalytic Properties of Proline-functionalized Pt-Nanoparticles

*Imke Schrader¹, Sarah Neumann¹, Rieke Himstedt¹, Alessandro Zana², Jonas Warneke¹, Sebastian Kunz^{*1}*

¹Institute for Applied and Physical Chemistry (IAPC), Faculty 2, University of Bremen, Leobenerstraße, 28359 Bremen, Germany

² Nano-Science Center, Department of Chemistry, University of Copenhagen, Universitetsparken 5, DK-2100 Copenhagen Ø, Denmark.

* Corresponding Author:

Dr. Sebastian Kunz

University of Bremen

Institute for Applied and Physical Chemistry (IAPC)

D-28359 Bremen

Tel: +49-421-218 63187

eMail: SebKunz@uni-bremen.de

1. Experimental Section

1.1 Material Preparation

1.1.1 Synthesis of “Unprotected” (Ethylene Glycol Stabilized) Pt Nanoparticles (NPs)

“Unprotected” Pt Nanoparticles NPs were prepared by a modified synthesis protocol established by Wang *et al.*¹ 0.25 g of $\text{H}_2\text{PtCl}_6 \times \text{H}_2\text{O}$ (40 wt% Pt, ChemPur) was dissolved in 25 ml ethylene glycol (EG, 99.8%, Sigma Aldrich). A solution of 0.50 g (for the synthesis of 1.2 nm large particles) or 0.125 g (2.1 nm particles) NaOH (98.9%, Fisher Chemical) in 25 ml EG was added under stirring at 500 rpm. An oil bath was preheated to 150 °C. The precursor solution was kept at 150 °C and a stirring rate of 500 rpm for 1.5 h to ensure complete reduction of the Pt precursor. The yellow precursor solution turned black after about 5 min, which indicates formation of Pt nanoparticles. The reaction mixture was cooled to ambient temperature and the particles were precipitated by adding 50 mL of 1 M HCl (VWR). The precipitated particles were separated from the supernatant solvent by centrifugation and washed once with 1 M HCl. The particles were then redispersed in 100 mL cyclohexanone ($\geq 99.0\%$, Sigma Aldrich).

1.1.2 Synthesis of Ligand-functionalized NPs

The preparation of ligand-functionalized Pt NPs followed a previously established phase transfer reaction for the functionalization of “unprotected” Pt NPs with hydrophilic ligands.² First an alkaline aqueous ligand solution was prepared with a ligand concentration of 8.3 mM and NaOH 12.5 mM. As ligands L-proline (> 99%, TCI), D-Proline (> 98%, TCI) and N-Methyl-L-proline (98%, Alfa Aesar) were used. In order to functionalize the NPs four aliquots of this ligand solution were added to the previously prepared dispersion of Pt NPs in cyclohexanone (see above). This gives a ligand to Pt ratio of 6.4 to ensure saturation of the particle surface with ligands. The resulting emulsion was stirred vigorously for 30 min. During this mixing the particles are functionalized and transferred from the organic phase into the aqueous phase, which was indicated by a colour change of both phases. The black aqueous ligand-Pt NP phase was separated from the organic phase in a separation funnel

1.1.3 Purification and Cleaning of Ligand-functionalized NPs

The aqueous dispersion of ligand-functionalized NPs was concentrated at a rotary evaporator ($p = 20$ mbar; $T = 40^\circ\text{C}$). The residue was precipitated by adding an excess of acetone (99.9 %, VWR). The precipitated functionalized particles were separated from the supernatant solvent by centrifugation and washed twice with ethanol (99.9 %, VWR).

1.2 Characterization

1.2.1 Determination of Ligand Coverage

The nitrogen content of each sample was determined using elemental analysis (EA) and the Pt content with atomic absorption spectroscopy (AAS). From these two measurements the nitrogen to Pt ratio was determined and used to estimate the ligand coverage by taking the particle size into account. The calculation of the dispersion (ratio of surface to total number of atoms) based on the average particle diameter has been previously described in more detail.² Preparation and cleaning of PRO-functionalized NPs was performed as described in 8.1.3. After cleaning the sample was dried for 12 h in a desiccator under reduced pressure. EA measurements were performed using a Euro ES elemental analyser with chromatographic separation and a TCD. AAS was conducted on a Carl Zeiss Technology AAS 5 FL spectrometer.

1.2.2 Deposition of “Unprotected” and Functionalized Particles

For catalytic investigations the “unprotected” and functionalized NPs were deposited onto Al_2O_3 (PURALOX SCCa 150/200; Sasol, grain size = 200-500 microns). The support material was added to the particle dispersions to give nominal metal loadings of 2 wt%. The solvent was removed using a rotary evaporator ($T = 60^\circ\text{C}$ for “unprotected and $T = 40^\circ\text{C}$ for functionalized particles; $p = 20$ mbar). In order to clean the supported Pt NPs, the functionalized samples were rinsed twice with ethanol (99.9 %, VWR) and the “unprotected” samples were rinsed twice with acetone (99.9 %, VWR). The cleaned catalysts were dried at reduced pressure and then immediately used for catalytic experiments.

The actual metal loading of every supported particle catalysts was measured by atomic absorption spectroscopy and used for normalization of the reaction rates.

1.2.3 IR Spectroscopic Characterization of PRO-functionalized Pt NPs

Spectra were recorded at an evacuable Vertex 80v Bruker spectrometer at a resolution of 4cm^{-1} and taking 100 scans. Before recording spectra the sample compartment of the spectrometer was evacuated for 6 min to remove residual gas-phase water and CO_2 . Measurements were performed on silicon wafer used as substrate for the functionalized particles. First, a clean silicon wafer was scanned and the obtained spectrum taken as the background for the sample measurement. Second, PRO-functionalized NPs prepared and purified as described in 8.1 were redispersed in deionized H_2O and deposited onto the silicon wafer via drop-casting. Thus supported particles were dried in an oven at $80\text{ }^\circ\text{C}$ for 20 min, then placed in the spectrometer and measured after evacuating for 6 min.

The Si-supported PRO-Pt NPs were then placed in an autoclave and exposed to the same experimental conditions applied for the catalytic studies (see 8.3). Afterwards the sample was removed from the reaction mixture and dried in a desiccator for 1 h under reduced pressure (20 mbar) prior to recording the spectrum.

1.2.3 TEM Investigations of NPs

Samples were prepared by drop-casting of the particle dispersion onto the TEM grid (ultrathin carbon film, Quantifoil, Cu 200 mesh). The grids were then dried in an oven for 30 min at $80\text{ }^\circ\text{C}$. Images were taken at a T20 G2 (Philips FEI, Oregon, USA) equipped with a thermionic electron gun operated at 200 eV. The micrographs were acquired using a Gatan 2K UltraScan 1000 CCD camera. Particle sizes were determined using ImageJ and counting at least 200 particles. From the average size the dispersion (ratio of surface atoms to total number of atoms within the particle) was estimated according to a model calculation previously described in detail.²

1.3 Catalytic studies

1.3.1 Catalytic Hydrogenation of Ethyl Acetoacetate (EAA)

The hydrogenation experiments were carried out at 25 °C in five in-house designed autoclaves. The autoclaves were connected to the same H₂ gas line and thermostat in order to perform five catalysis experiments under identical experimental conditions.

200 mg catalyst were added to a solution of 1 ml ethyl acetoacetate (Aldrich, ≥99,0 %) and 9 ml tetrahydrofuran (VWR, 100%). Before reaction the autoclaves were flushed three times with H₂ (Linde 5.0). The experiments were performed at a reaction pressure of 20 bar and a stirring speed of 800 rpm. For reaction rate measurements the conversion was kept below 10 % to achieve differential operation conditions. After a reaction time (30 min) the catalyst was removed by centrifugation and the product was analysed.

The conversion was tested to scale linearly with the amount of catalyst used within the experiment. Control experiments by varying the stirring rate as well as the catalyst pellet size by grinding the supported particles did not affect the obtained conversions, confirming that experiments are performed in the absence of any diffusion limitations.³

All enantiomeric excesses (ee) reported in the manuscript were determined from experiments with turnover numbers (TON) that were low enough to exclude suitable changes of stereoselectivity by alteration of the catalyst (see long-term stability tests in Section 8).

1.3.2 Product Analysis of Catalytic Experiments

Conversion and enantiomeric excess of the catalytic experiments were analysed using a gas chromatograph (Shimadzu GC-2010plus AF IVD) equipped with a flame ionization detector (FID). A column flow of 0.86 ml min⁻¹ was applied with He (Linde, 5.0) as carrier gas and a linear velocity of 25.1. cm s⁻¹. For analysis 500 µL sample was diluted with 500 µL acetone (VWR, 99.9 %). Injection was performed at 200°C with a split ratio of 50:1.

To determine the conversion a VSD (SGE, 2 m length, 320 µm inner diameter, 430 µm film

thickness) column was used. The column was held at 110°C for 8 min, ramped at 20°C/min to 180°C, and then held 1 min at this temperature, before the temperature program was stopped.

The enantiomeric excess was determined using a Lipodex E (Macherey-Nagel, 27 m length, 0.25 mm inner diameter, 0.25 μ m film thickness) column. Prior to analysis the reaction product was derivatized using N-Methylbis(trifluoroacetamid). 20 μ L reagent was added to the diluted sample and the mixture was left at 60 °C for 3h. The oven temperature was held at 85°C for 15 min, then heated to 180°C at a rate of 30 °C min⁻¹ and kept for 10 min. Then the temperature program was stopped. Representative chromatogram is shown in Fig. S7 demonstrating proper separation of the signals of the two product enantiomers.

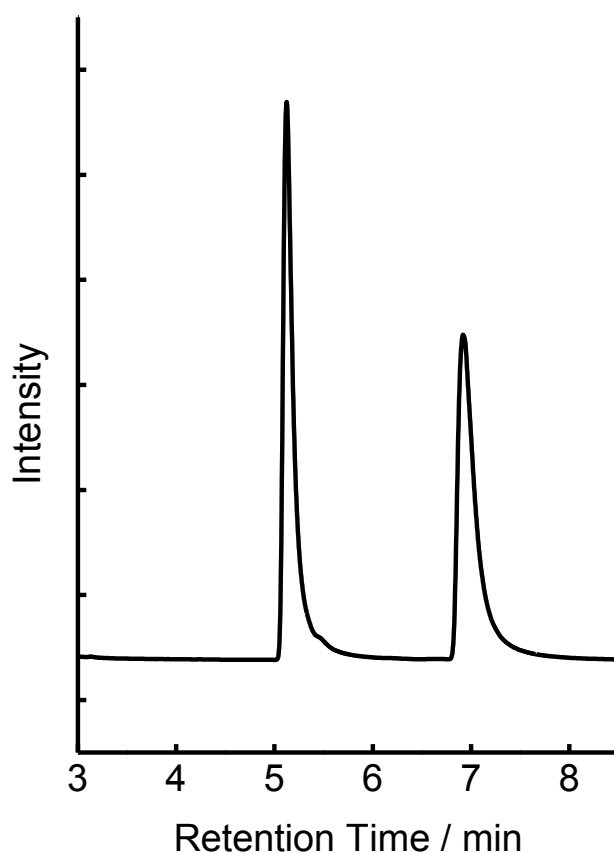


Figure S1. Representative chromatogram illustrating the separation of the two product enantiomers (t_r =5.131min and 6.995min, see 1B and C in Fig. 1 for structures).

In order to determine the product configuration, Ethyl (*R*)-(-)-3-Hydroxybutyrate (1C in Fig. 1, TCI, > 98 %) was purchased and analyzed after derivatization as described above.

The activity and selectivity were determined from the total amount of detected product and reactant and by taking the corresponding response factors into account.^{4,5} The experimental errors of the stereoselectivities and activities were determined from the standard deviation of five catalysis experiments.

1.3.3 Testing for Desorption of Ligands into Reaction Medium in Long-term Applications via Electrospray Ionization Mass Spectrometry (ESI-MS)

Electrospray Ionization Mass Spectrometry (ESI-MS) measurements were performed on a Bruker Esquire-LC ion trap mass spectrometer. One droplet of the product mixture was dissolved in 450 μ L methanol. The solution was injected into the mass spectrometer via a syringe pump at a flow rate of 3 mL min⁻¹. Spectra were recorded in the positive and negative ion mode for one minute and averaged.

2. Particle Size Analysis of Small and Large Pt NPs

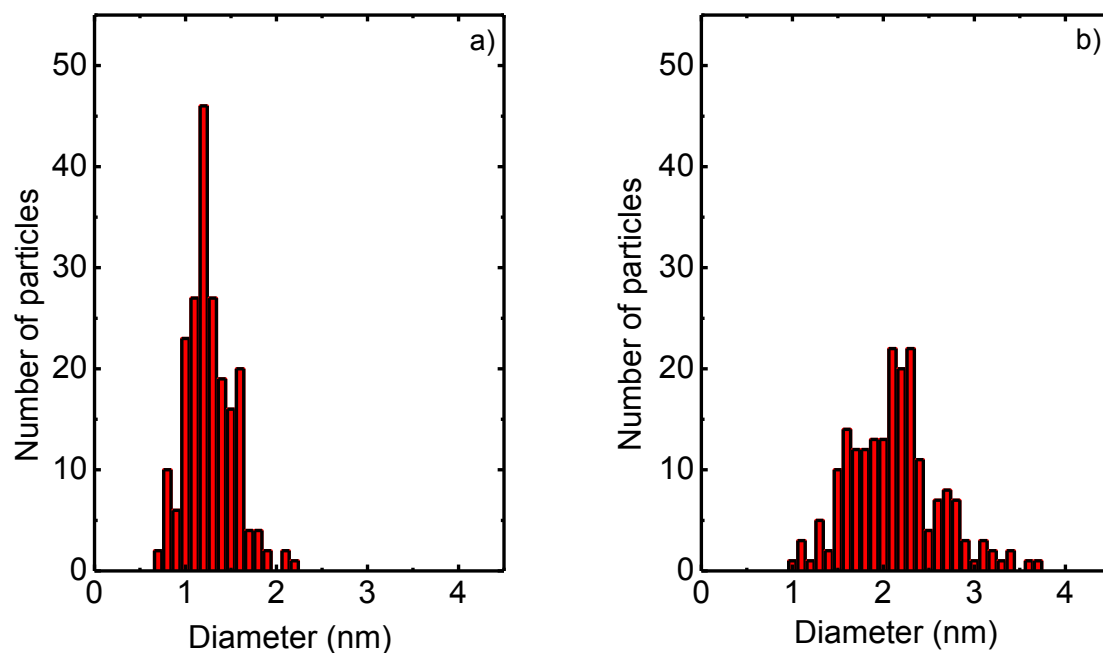


Figure S2. Particle size distributions of 1.2 nm large (a) and 2.1 nm large PRO-functionalized Pt NPs (b).

Particle size distributions of 1.2 ± 0.3 nm (Fig. S2a) and 2.1 ± 0.5 nm large (Fig.S2b) Pt NPs functionalized with PRO, determined from TEM images using open source software ImageJ and counting at least 200 particles. Representative TEM images are shown in Figure S3. As previously reported no sintering was observed after functionalization and the particle size was maintained.

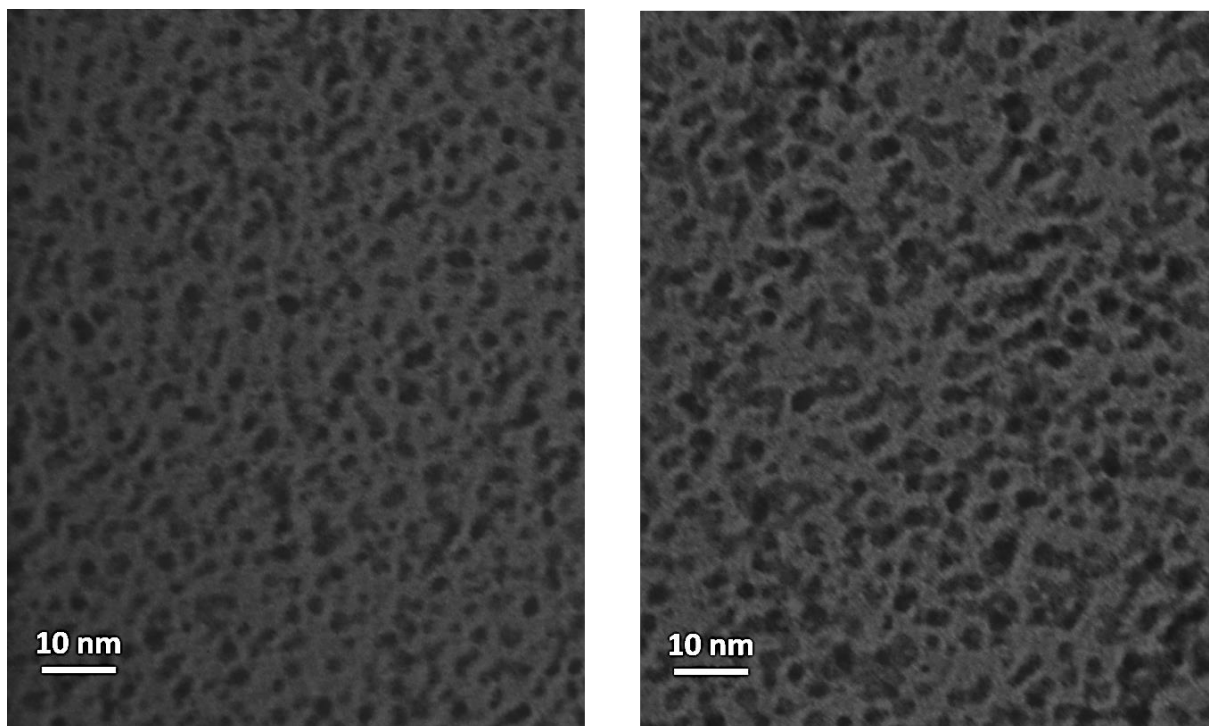


Figure S3. Representative TEM images of particles investigated in the present study. Small particles (1.2 ± 0.3 nm) are shown on the left, the larger particles (2.1 ± 0.5 nm) on the right. Due to the high NP loadings areas of aggregated NPs can be identified. Zooming into these aggregates however reveals that they consist of isolated NPs that are not sintered.

3. Calculation of Atoms with Different Numbers of Neighbors for Two Different Particle Sizes

In order to calculate the number of atoms in a specific position and with a specific number of neighbours for the two particles, an idealized f.c.c. cubo-octahedron structure was assumed. The Pt particle sizes determined by TEM are about 1.2 and 2.1 nm, which corresponded approximately to 64 and 340 atoms, respectively, by taking a Pt radius of 0.136 nm into account and assuming a spherical shape.² According to the model of van Hardeveld and Hartog⁶ the number of atoms in specific position were calculated based on Table S1. C_6 describes the corner atoms with six nearest neighbours. C_7 describes the atoms on the edges with seven nearest neighbours and C_8 and C_9 plain atoms with eight/nine nearest neighbours.

Table S1. Calculation of atoms in a specific position and with a specific number of neighbors. M being the number of atoms lying on an equivalent edge (corner atoms included). N_T total numbers of atoms. N_B number of bulk atoms. N_S number of surface atoms. With a particle size of 64 and 340 atoms m is calculated to be 2.26 and 3.448. For further details see reference.⁶

	Equation	$m= 2.26$	$m= 3.448$
N_T	$16m^3-33m^2+24m-6$	64.38	340.30
N_B	$16m^3-63m^2+84m-38$	14.75	158.52
N_S	$30m^2-60m+32$	49.63	181.78
C_6	24	24	24
C_7	$12(m-2)+24(m-2)$	9.36	52.13
C_8	$6(m-2)^2$	0.41	12.58
C_9	$8(3m^2-9m+7)$	15.86	93.07
Corner-atoms	C_6	24	24
Edge-atoms	C_7	9.36	52.13
Plain-atoms	C_8, C_9	16.27	105.65

4. IR Spectroscopic Investigation of L-proline-functionalized Pt NPs Before and After Exposure to Catalytic Conditions

In order to demonstrate qualitatively the formation of CO during carbonyl hydrogenation IR spectra of PRO-Pt NPs before and after exposure to catalytic conditions were taken (see Fig. S4). Spectra were shifted in order to achieve a better illustration.

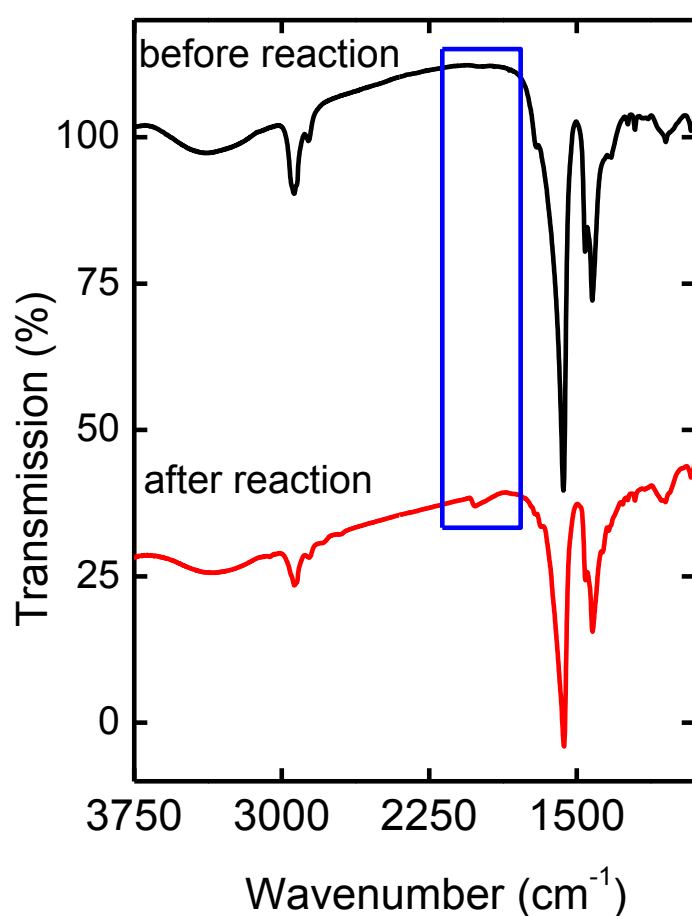
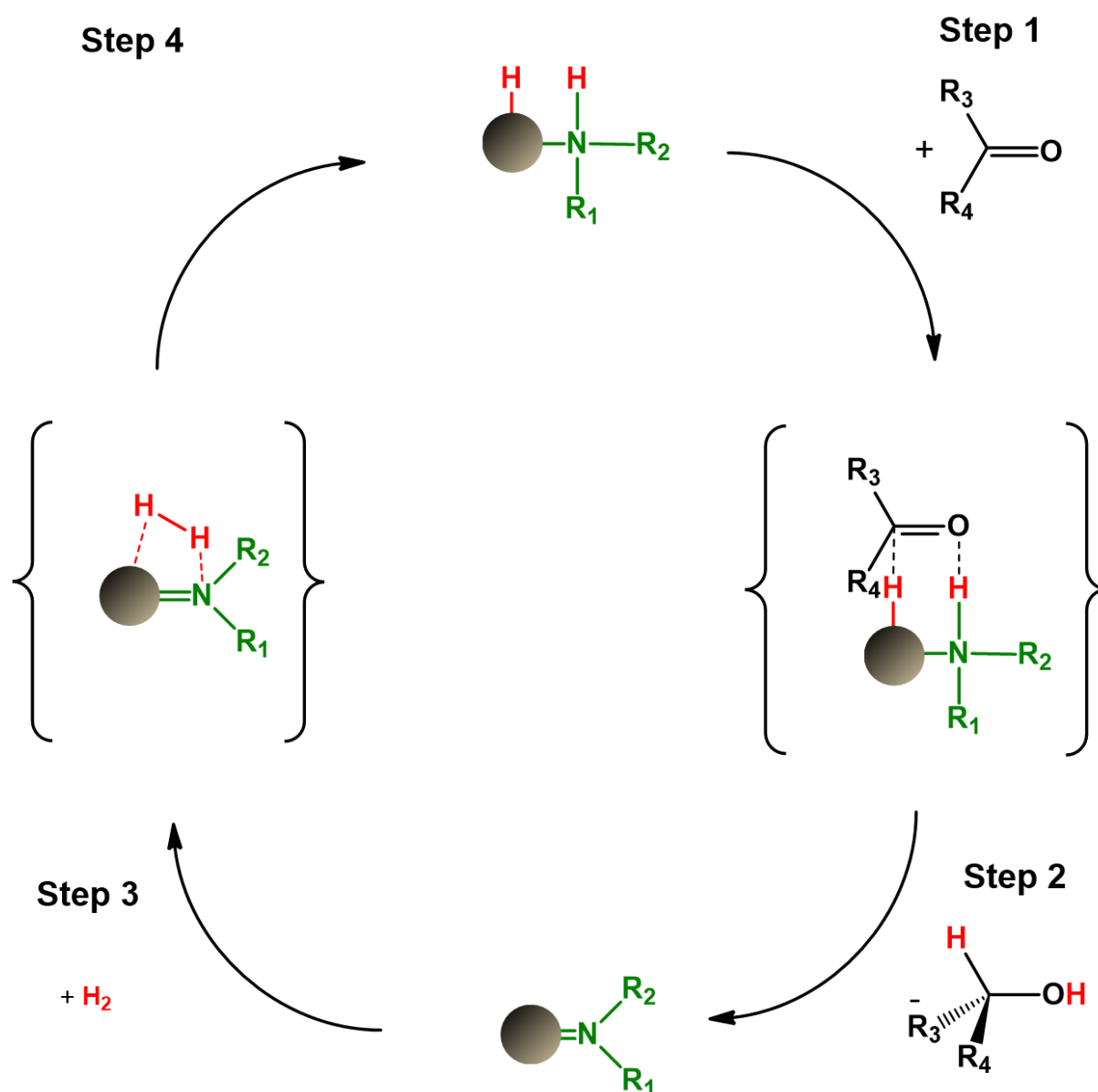


Figure S4. IR spectra of L-PRO-Pt before (black) and after exposure to catalytic conditions (red). After catalytic conditions the PRO-Pt NPs show a feature at 2016 cm⁻¹ that can be related to CO adsorbed on isolated Pt sites.

Comparison of the two spectra reveals that all features that can be seen before exposure to catalytic conditions also appear for the sample after exposure. However, after catalysis an additional feature

appears at around 2016 cm^{-1} (see blue box). This band is characteristic for CO on isolated Pt sites³ supporting the hypothesis of CO formation via decarbonylation.⁷

5. Ligand-accelerated Hydrogenation of Carbonyls via N-H Effect



Scheme S1. Ligand-accelerated hydrogenation of carbonyls via N-H effect. The C=O reactant interacts with hydrogen that is bound to the metal centre and an amine bound proton, to become activated (Step 1) and hydrogenated (Step 2). The catalyst is reformed by coordinating molecular hydrogen (Step 3) that is then heterogeneously dissociated by interacting with a ligand-free surface atom and the ligand nitrogen (Step 4).

The N-H assisted catalytic cycle, known from homogenous catalysis (Scheme S1), proposes that through coordination of primary and secondary amines to a late transition d-metal (grey sphere) the amine bound hydrogen becomes acidic.⁸ This allows a reaction pathway in which a proton is transferred from the amine to the carbonyl oxygen (Step 1) and a hydride from the metal to the

carbonyl carbon, leading to an enhanced hydrogenation rate (Step 2). After reaction the product desorbs and the catalyst adsorbs (Step 3) molecular H_2 that is heterogeneously dissociated (Step 4) by which the active catalyst is reformed.⁸

6. Formation Rates of “Unprotected”, D- and L-proline-functionalized Pt NPs vs. N-Methyl-L-PRO functionalized Pt NPs

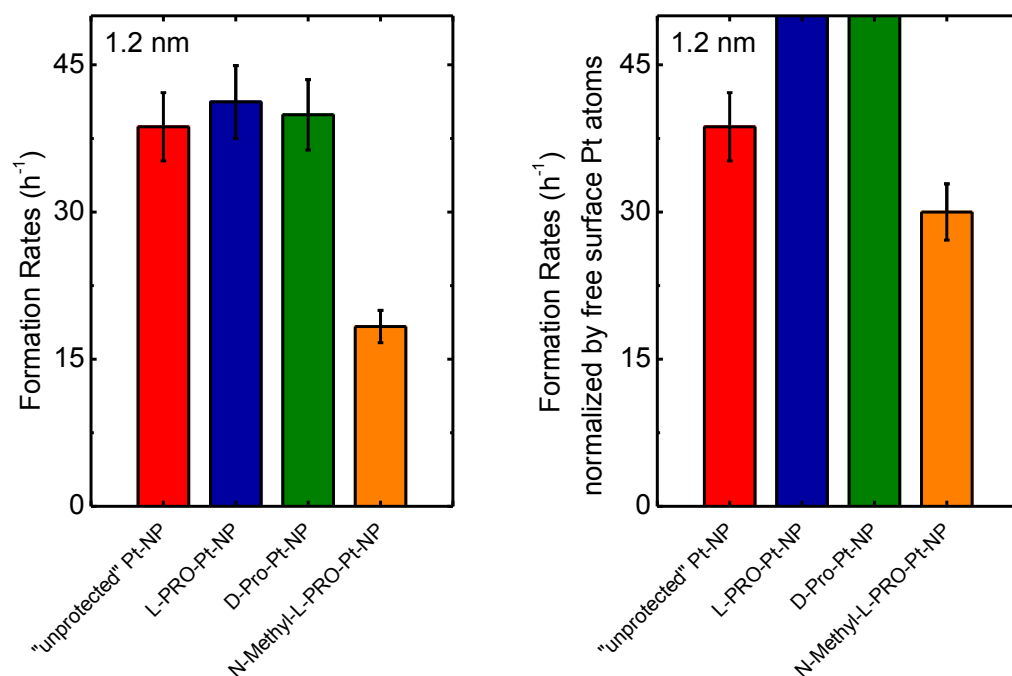


Figure S5. Formation rates normalized to the total number of surface atoms (left) and to the number of ligand-free surface atoms (right) over “unprotected” (red), L-PRO-Pt (blue), D-PRO-Pt (green), and N-Methyl-L-PRO-Pt NPs (yellow) with a size of 1.2 nm.

The formation rates obtained from catalysis experiments performed with supported “unprotected”, L-PRO-Pt, D-PRO-Pt, and N-methyl-L-PRO-Pt NPs demonstrate that the binding of the tertiary amine (N-methyl-L-PRO) leads to an inhibition of the catalytic activity (Fig. S5 left). In order to account for the fact that the activity is limited by the availability of ligand-free surface atoms, the formation rates were also normalized to the total number of ligand-free surface atoms (Fig. S5 right). For N-methyl-L-PRO-functionalized NPs a ligand coverage of 0.4 was used as determined by TEM, EA, and AAS and previously reported.⁹ After this correction the rate over the N-methyl-L-PRO-functionalized NPs is still slightly lower than that over “unprotected” Pt NPs. In contrast, the rates of L- and D-proline-functionalized NPs exceed significantly the activity of “unprotected” after normalization to the number of ligand-free surface atoms (see Fig. S6 for a different y-scale that shows the actual rates over PRO-functionalized NPs, ligand coverages are given in Table 1). This shows that

in contrast to N-methyl-PRO, L- and D-proline lead to an activity enhancement when considering that ligand-free surface atoms are required to obtain catalytic activity and evidences the relevance of N-H for this enhancement effect.¹⁰

7. Formation Rates Normalized to the Total Number of Ligand-free Surface Atoms

In order to illustrate the effect of ligand acceleration the formation rates normalized to the total number of ligand-free surface atoms are shown in Figure S6. The two graphs show the same data but with different y-scaling in order to achieve a better illustration for comparison of the different samples.

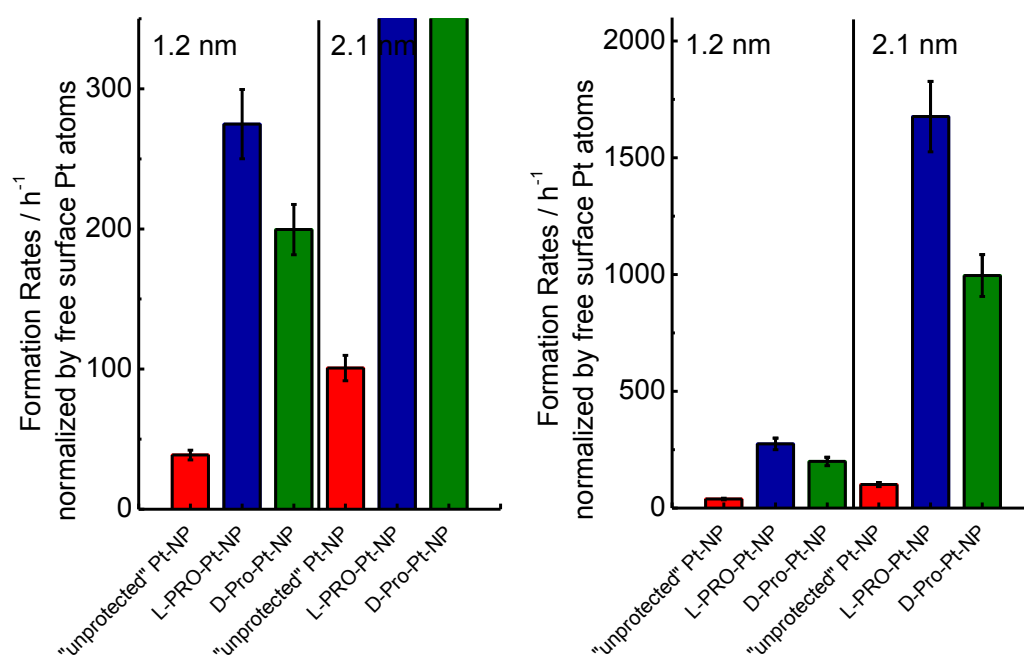


Figure S6. Formation rates over “unprotected”, L-PRO-Pt, and D-PRO-Pt normalized¹⁰ to the total number ligand-free surface Pt atoms. The two graphs show the same data but at different y-scaling.

The results demonstrate that the formation rates over PRO-Pt NPs are significantly higher than that over “unprotected” Pt NPs. The difference between the rates over small and large PRO-functionalized NPs can be explained by partial poisoning through CO as already discussed in more detail in the manuscript. Low coordinated surface atoms perform decarbonylation which leads to poisoning of these sites by CO.³ The number of low to highly coordinated surface atoms is lower on larger particles. As a consequence larger particles show less CO poisoning.

In order to obtain rates normalized the number of ligand-free surface atoms, the rates shown in Figure 2 have to be divided by 1 minus the ligand coverages. This means that small uncertainties in

the experimental determination of the ligand coverage lead readily to significant changes of the values required for the normalization to obtain Figure 6 from Figure 2. As the rates normalized to the total number of surface atoms of particles of the same size but functionalized with either L- or D-PRO were found to be very similar (see Fig.2 in the manuscript), we assume that the differences in the rates in Figure S6 are merely the result of normalizing the rates (from Fig. 2) by a small number with a relatively high uncertainty. Therefore the obtained difference of the rates shown in Figure S6 for particles of the same size but with ligands of different configurations should not be further stressed.

8. Long-term Catalytic Test

The results of catalytic long-term experiments performed with supported PRO-Pt NPs demonstrate that the stereoselectivity is constant over more than 220 turnovers (TONs) per ligand (Figure S7). At higher TONs changes of the actual catalyst have to be considered as the stereoselectivity starts to decrease.

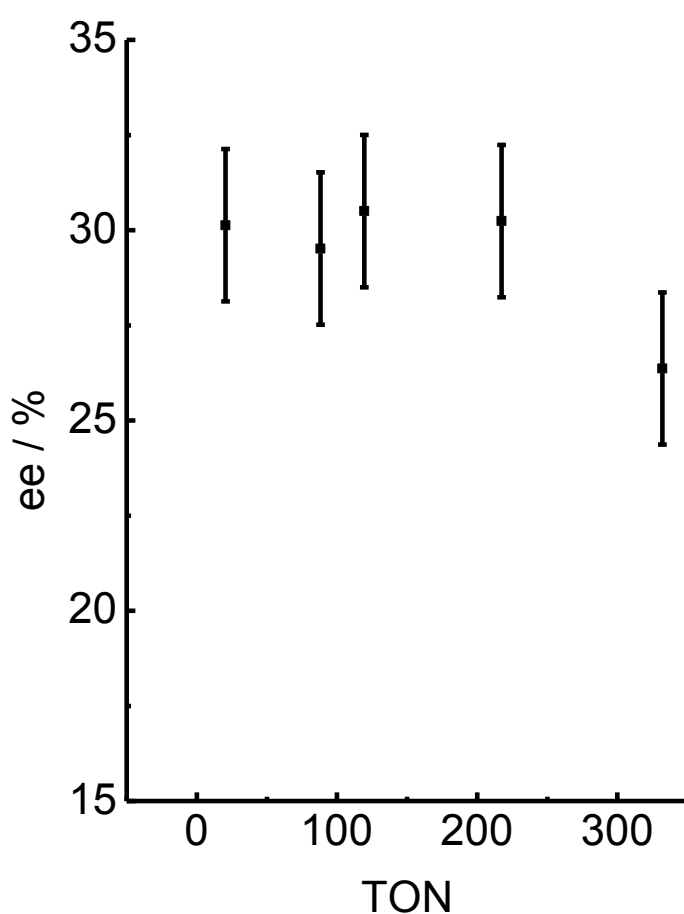


Figure S7 Catalytic long-term experiment performed with supported L-PRO-Pt NPs in THF

As the ligand is the chiral element of the catalyst, we relate the decrease of the stereoselectivity to a loss of surface bound ligands. Two scenarios can be envisioned to induce a fade of surface bound ligands. Either the ligands diffuse from the particle onto the support (spillover) or the increasing polarity of the reaction medium (alcohols are continuously formed at the expense of

ketones) leads eventually to a slight solubility of the ligand in the liquid bulk, which causes ligand desorption. While the first is difficult to probe, the latter can be investigated by analysing the composition of the reaction medium via mass spectrometry (see 1.3.3). Tests performed with reaction media from long-term experiments for which a loss of stereoselectivity was obtained revealed no evidence for PRO dissolved in the reaction medium. We hence assume that the decrease of stereoselectivity for increasing reaction periods is related to spillover and not to ligand desorption into the liquid bulk.

9. References

- (1) Wang, Y.; Ren, J. W.; Deng, K.; Gui, L. L.; Tang, Y. Q. *Chem. Mater.* **2000**, *12*, 1622.
- (2) Kunz, S.; Schreiber, P.; Ludwig, M.; Maturi, M. M.; Ackermann, O.; Tschurl, M.; Heiz, U. *Phys. Chem. Chem. Phys.* **2013**, *15*, 19253.
- (3) Singh, U. K.; Vannice, M. A. *Applied Catalysis A: General* **2001**, *213*, 1.
- (4) Scanlon, J. T.; Willis, D. E. *J. Chromatogr. Sci.* **1985**, *23*, 333.
- (5) Holm, T. *Journal of Chromatography A* **1999**, *842*, 221.
- (6) Van Hardeveld, R.; Hartog, F. *Surf. Sci.* **1969**, *15*, 189.
- (7) Altmann, L.; Kunz, S.; Bäumer, M. *J. Phys. Chem. C* **2014**, *118*, 8925.
- (8) Clapham, S. E.; Hadzovic, A.; Morris, R. H. *Coord. Chem. Rev.* **2004**, *248*, 2201.
- (9) Schrader, I.; Warneke, J.; Backenköhler, J.; Kunz, S. *J. Am. Chem. Soc.* **2015**, *137*, 905.
- (10) Noyori, R.; Ohkuma, T. *Angew. Chem., Int. Ed.* **2001**, *40*, 40.